Cholinergic filtering in the recurrent excitatory microcircuit of cortical layer 4

Emmanuel Eggermann[a,1] and Dirk Feldmeyer[a,b]

[a]Institute of Neuroscience and Medicine, INM-2, Research Centre Juelich, D-52425 Juelich, Germany; and [b]Department of Psychiatry and Psychotherapy, and Juelich-Aachen Research Alliance-Brain, Translational Brain Medicine, Rheinisch-Westfaelische Technische Hochschule Aachen University, D-52074 Aachen, Germany

Edited by Bert Sakmann, Max-Planck-Institut, Martinsried, Germany, and approved May 29, 2009 (received for review October 14, 2008)

Neocortical acetylcholine (ACH) release is known to enhance signal processing by increasing the amplitude and signal-to-noise ratio (SNR) of sensory responses. It is widely accepted that the larger sensory responses are caused by a persistent increase in the excitability of all cortical excitatory neurons. Here, contrary to this concept, we show that ACH persistently inhibits layer 4 (L4) spiny neurons, the main targets of thalamocortical inputs. Using whole-cell recordings in slices of rat primary somatosensory cortex, we demonstrate that this inhibition is specific to L4 and contrasts with the ACH-induced persistent excitation of pyramidal cells in L2/3 and L5. We find that this inhibition is induced by postsynaptic M_4-muscarinic ACH receptors and is mediated by the opening of inwardly rectifying potassium (K_{ir}) channels. Pair recordings of L4 spiny neurons show that ACH reduces synaptic release in the L4 recurrent microcircuit. We conclude that ACH has a differential layer-specific effect that results in a filtering of weak sensory inputs in the L4 recurrent excitatory microcircuit and a subsequent amplification of relevant inputs in L2/3 and L5 excitatory microcircuits. This layer-specific effect may contribute to improve cortical SNR.

acetylcholine | muscarinic receptors | sensory cortex | synaptic transmission

Our sensory perceptions are dramatically enhanced when we wake up and become maximal during periods of sustained attention. It is believed that acetylcholine (ACH) plays an important role in this enhancement. Indeed, the neocortical ACH concentration specifically increases during wakefulness and periods of sustained attention (1, 2). Furthermore, iontophoresis of ACH in the neocortex of anesthetized animals (3–5) produces an increase in amplitude and signal-to-noise ratio (SNR) of evoked sensory responses similar to those occurring after transition from sleep to wakefulness (6). Conversely, experimental lesions of cholinergic neurons in the basal forebrain (7), the major source of neocortical ACH, or genetically induced reduction of ACH release (8) lead to impaired sensory processing.

To understand the mechanism whereby ACH modulates cortical processing, several in vitro studies examined its effect on neocortical excitatory neurons. These studies showed that ACH invariably induces a persistent increase in the excitability of pyramidal cells (PCs) through activation of postsynaptic muscarinic ACH receptors (mAChRs) (9–12), even though in 2 particular experimental conditions (10, 12) puff applications of ACH evoke a transient (≈1 s) hyperpolarization preceding or superimposed on a persistent depolarization. Neocortical nicotinic AChRs mainly found on axon terminals have been shown to enhance synaptic transmission (13). Thus, it is currently held that the cholinergic enhancement of sensory processing results from a persistent increase in the excitability of all neocortical excitatory neurons (14–16). However, while such an increase can explain the larger amplitude of the evoked cortical sensory responses observed in vivo during high levels of intracortical ACH, it does not account for their increased SNR. The finding that presynaptic AChRs selectively enhance sensory inputs over cortico-cortical feed-back inputs (17–19) has led to the hypothesis that such a mechanism could underlie the increase in SNR (14).

Although the action of ACH has been extensively studied in neocortical PCs, its effects on identified excitatory neurons in layer 4 (L4) have not been investigated. In the primary somatosensory cortex (S1), these neurons form a recurrent excitatory microcircuit largely restricted to a single cortical column (20). They directly receive the majority of thalamocortical afferents and have therefore a key position in the cortical network. In addition to their gating function, they are also believed to reinforce thalamocortical inputs before activating L2/3-PCs (21, 22). Thus, modulation of L4 excitatory neurons should have important consequences for cortical sensory processing.

The aim of this study was to examine the effects of ACH on intrinsic membrane properties and on synaptic transmission in the L4 excitatory neurons.

Results

Characterization of L4 Spiny Neurons in S1. Excitatory neurons of L4 in S1 cortex of rats, that is, spiny stellate and star pyramidal neurons, were identified using the following criteria (21): their localization inside the hollows or walls of the barrels, their small ($<$14 μm) rounded shape and their regular firing pattern preceded by an initial fast doublet of action potentials (APs). Since in our experiments the neurons showed homogeneous responses to ACH, we did not discriminate spiny stellate from star pyramidal neurons, and we will refer to them as "L4 spiny neurons" (L4-SN).

ACH Persistently Hyperpolarizes the L4 Spiny Neurons. Bath applications of 100 μM ACH hyperpolarized all L4-SNs tested ($n >$ 70 for P18–P24 rats; $n = 5$ for P36) at V_{rest} (Fig. 1*A*, *Upper*) or more depolarized potentials (V_{-60mV}, between −57 and −63 mV). ACH also reduced the amplitude of voltage deflections elicited by brief negative current injections (Fig. 1*A*, *Upper*) indicating a decrease in membrane resistance. The hyperpolarization was persistent, since it always lasted until the end of the ACH applications (up to 16 min; Fig. 1*A*, *Lower*).

The dose dependence of this effect was investigated by bath application of increasing concentrations of ACH (1 μM to 1 mM) on neurons held at V_{-60mV}. All neurons tested were significantly hyperpolarized by 1 μM of ACH and their responses increased with higher concentrations (Fig. 1*B*). A concentration for a half-maximum effect (EC_{50}) of 6.5 ± 0.5 μM was deter-

Author contributions: E.E. designed research; E.E. performed research; D.F. contributed new reagents/analytic tools; E.E. analyzed data; and E.E. and D.F. wrote the paper

The authors declare no conflict of interest.

This article is a PNAS Direct Submission.

[1]To whom correspondence should be addressed at: Department of Physiology, University of Freiburg, Engesserstrasse, 4, 79104 Freiburg, Germany. E-mail: emmanuel.eggermann@physiologie.uni-freiburg.de.

This article contains supporting information online at www.pnas.org/cgi/content/full/0810062106/DCSupplemental.

NEUROSCIENCE

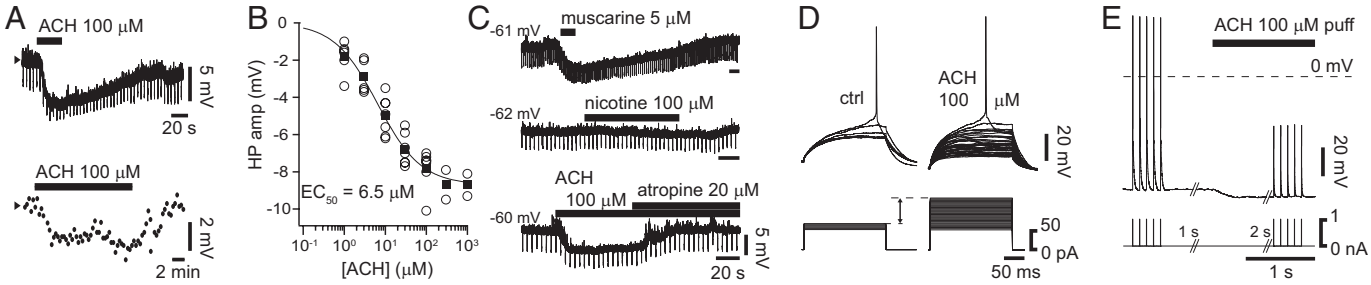

Fig. 1. Low concentrations of ACH persistently hyperpolarize L4-SNs in S1 by activating postsynaptic mAChRs. (*A*) *Upper*, bath application of 100 μM ACH hyperpolarizes a L4-SN recorded in current-clamp at V_{rest}. *Lower*, the hyperpolarization persists until the end of long bath applications (membrane potential is measured every 20 s). (*B*) The dose-response relationship of ACH in L4-SNs at V_{-60mV} is well fitted by the Hill equation. Note that 1 μM ACH always evokes a hyperpolarization. Open circles, individual values; filled boxes, mean values. (*C*) The hyperpolarization is mimicked by 5 μM muscarine (*Top*) but not by 100 μM nicotine (*Middle*); it is blocked by 20 μM atropine (*Bottom*). (*D*) The current threshold of a L4-SN increases (double-headed arrow) during bath application of 100 μM ACH (*Right*). (*E*) A puff of 100 μM ACH inhibits the firing of a L4-SN stimulated with trains of 5 × 5 ms intracellular suprathreshold stimuli.

mined by fitting the dose-response relationship with the Hill equation.

Next, we examined whether the hyperpolarization was a direct effect of ACH or whether it might result from the ACH-induced excitation of presynaptic GABAergic interneurons (12). Consecutive bath applications of 100 μM ACH in control conditions and in the presence of the sodium channel blocker tetrodotoxin (TTX, 1 μM), the $GABA_A$ receptor blocker gabazine (GBZ, 10 μM), and the $GABA_B$ receptor blocker CGP-35348 (1 μM) were not significantly different in neurons held at V_{-60mV} (−6.7 ± 0.5 mV vs. −6.9 ± 0.5 mV; $P = 0.67$; $n = 7$). Furthermore, similar responses were observed in a high magnesium (10–16 mM)/low calcium (0.1 mM) solution ($n = 6$). These results demonstrate that the hyperpolarization is elicited by the activation of postsynaptic ACHRs.

To determine which type of ACHRs was activated, we tested the effect of cholinergic agonists on neurons held at V_{-60mV}. Muscarine (5 μM) induced a hyperpolarization (−8.7 ± 0.8 mV, $n = 7$; Fig. 1*C*, *Top*) similar to that of saturating concentrations of ACH (Fig. 1*B*), but 100 μM nicotine had no significant effect (−61.5 ± 0.4 mV, vs. −62.1 ± 0.4 mV; $n = 7$; $P = 0.16$; Fig. 1*C*, *Middle*). Consistent with the effect of muscarine, 10–20 μM atropine completely blocked (102.5 ± 2.1%, $n = 10$) the hyperpolarization induced by 100 μM ACH (Fig. 1*C*, *Bottom*). Thus, the hyperpolarization is induced by the activation of mAChRs.

The ACH-induced hyperpolarization and reduction in input resistance should decrease the excitability of L4-SNs. To quantify this effect, we used current steps of increasing amplitudes before, during and after bath application of ACH. ACH (100 μM) reversibly increased the current threshold of the tested neurons to 147 ± 10% of control values ($P < 0.01$, $n = 8$; Fig. 1*D*). When 10 μM ACH was applied to a subset of these neurons, the current threshold was similarly increased (+167 ± 11%, $P < 0.05$, $n = 3$). For both concentrations, ACH had no effect on the AP threshold (−33.6 ± 1.1 mV, vs. −33.1 ± 1.2 mV; $P = 0.23$; $n = 8$).

To assess the physiological significance of the ACH-induced persistent inhibition, we performed long-lasting puff applications of ACH on L4-SNs stimulated with trains of 5 short suprathreshold current injections at 10 Hz. Such stimuli resemble the S1 thalamocortical inputs coming from the whiskers in awake animals (23, 24). The firing elicited during the train in control conditions was abolished during application of 100 μM ACH (Fig. 1*E*; $n = 3$). Thus, during periods of increased neocortical ACH release, the lower responsiveness of L4-SNs can reduce the impact of small sensory inputs, suggesting a filtering action of ACH in the L4 recurrent excitatory microcircuit.

Although the present study focuses on S1 cortex, we found that ACH also persistently hyperpolarizes L4-SNs in the primary auditory (A1) and visual (V1) cortex (Fig. S1), suggesting that the ACH-induced persistent inhibition of L4-SNs is a general feature of the sensory cortices.

The Persistent Hyperpolarization Is a Specific Feature of L4. The ACH-induced persistent hyperpolarization described here is in marked contrast to the ACH-induced persistent depolarization previously demonstrated in identified neocortical PCs (9–12). Therefore, it is likely that this type of response is a unique feature of L4-SNs. To investigate this possibility further, we compared the responses of excitatory neurons at V_{rest} in L2/3, L4, and L5 to puff applications of 100 μM ACH (Fig. 2*Ai*, *Bi*, and *Ci*). We found that such applications induced a hyperpolarization in all L4-SNs tested ($n = 37$; Fig. 2*Bii*) and a depolarization in all L2/3 ($n = 15$; Fig. 2*Aii*) and L5 ($n = 18$; Fig. 2*Cii*) PCs tested. These responses were persistent since they lasted until the end of long (10 s) puff applications ($n = 5$ for L2/3; $n = 4$ for L4; $n = 6$ for L5; Fig. 2*Aii*, *Bii*, and *Cii*). Although the persistent depolarization was accompanied by a transient hyperpolarization (*Insets* in Fig. 2*Aii* and *Cii*) in one-third of the L2/3 PCs (5/15) and half of the L5 PCs (9/18), this transient hyperpolarization represented only a minor part of the biphasic effect of ACH, both in duration and amplitude, even for 1-s puff applications (Fig. 2*Aiii* and *Ciii*). Thus, the effect of ACH is not only layer-specific in S1, but it also differentially modulates the major thalamocortical input layer and the more integrative layers.

The Persistent Hyperpolarization Is Induced by M_4R. Since the ACH-induced persistent depolarization and transient hyperpolarization of PCs are mediated by the activation of M_1-subtype of mAChRs (M_1Rs) (10, 25), we tested whether the persistent hyperpolarization of L4-SNs might be of the same origin. Although 0.5 μM pirenzepine (PIR), a M_1Rs-selective antagonist, completely blocked the transient hyperpolarization evoked by puff applications of 100 μM ACH on L5 PCs ($n = 3$), it only partially blocked (66.7 ± 5%, $n = 9$) the persistent hyperpolarization in all L4-SNs (Fig. 3*A*). This could indicate that the response is mediated in part by a different mAChR subtype. Likely candidates are M_2Rs and M_4Rs, since they are generally linked to an inhibitory pathway via $G_{i/o}$ proteins. Thus, we tested methoctramine (MTA) at 0.5 or 1 μM, a selective M_2Rs antagonist, and tropicamide (TRO) at 1 μM, a selective M_4Rs antagonist. While MTA had no effect (Fig. 3*B*), TRO completely blocked the persistent hyperpolarization in 5 out of 11 neurons (Fig. 3*C*) and partially blocked it in the others (mean block for all cells 90.3 ± 3%, $n = 11$). Because i) the mean TRO block is stronger than the mean PIR block and ii) only TRO can completely block the response, we hypothesized that the hyper-

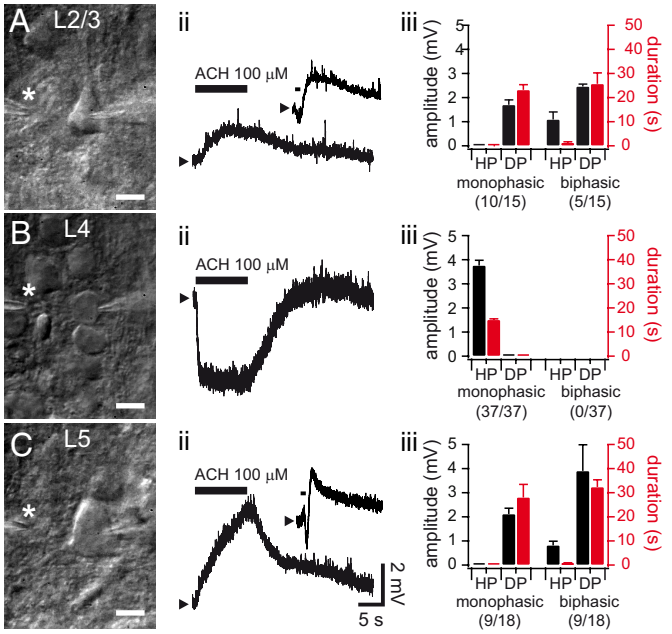

Fig. 2. Differential layer-specific effect of ACH. ACH persistently depolarizes PCs in L2/3 (*A*) and L5 (*C*), but persistently hyperpolarizes the L4-SNs (*B*). Column i, high magnification image of a L2/3 PC (*Ai*), a L4-SN (*Bi*), and a L5 PC (*Ci*). Asterisks show the tip of the puff electrode. (Scale bars, 10 μm.) Column 2, a 10-s puff of 100 μM ACH persistently depolarizes a L2/3 PC (*Aii*), persistently hyperpolarizes a L4-SN (*Bii*), and persistently depolarizes a L5 PC (*Cii*). *Insets*, 1 s puffs evoke a biphasic response in some L2/3 and L5 PCs. Voltage traces are averages from 3 consecutive trials in neurons at V_{rest} (arrowheads). Column 3, summary of the mean amplitude (black bars) and duration (red bars) of hyperpolarization (HP) and depolarization (DP) in response to 1-s puffs of 100 μM ACH in L2/3 PCs (*Aiii*), L4-SNs (*Biii*), and L5 PCs (*Ciii*). The left part of each histogram reports the monophasic responses and the right part the biphasic ones.

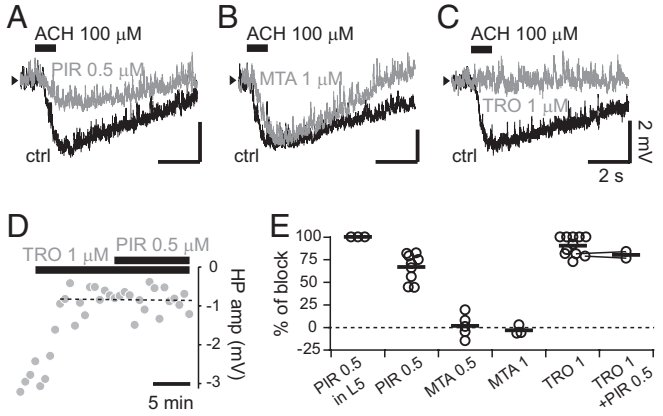

Fig. 3. The persistent hyperpolarization is induced by M_4R. While pirenzepine (PIR) at 0.5 μM only partially blocks (gray trace) the persistent hyperpolarization evoked by 1-s puffs of 100 μM ACH in control (black trace) (*A*), methoctramine (MTA) at 1 μM has no effect (*B*) and tropicamide (TRO) at 1 μM blocks it (*C*). (*D*) In a neuron wherein the persistent hyperpolarization was not completely blocked by 1 μM tropicamide (TRO), 0.5 μM pirenzepine (PIR) has no additional effect. The graph shows the time-course of the amplitude of the persistent hyperpolarization (HP amp) evoked by 1-s puffs of 100 μM ACH. Dashed line is a linear fit obtained from the adjacent points. (*E*) Summary plot showing the percentage of block of the different antagonists. Lines between points indicate occlusion experiments. Concentrations are in μM. Voltage traces are averages from 3 successive puffs and were Y-aligned. Arrowheads indicate V_{rest}.

polarization was induced by the activation of M_4Rs only and that PIR had an unspecific effect on these receptors (26). Accordingly, application of 1 μM TRO + 0.5 μM PIR on 2 neurons that were not completely blocked by 1 μM TRO showed no additive antagonism (Fig. 3*D*). These pharmacological experiments (summary in Fig. 3*E*) indicate that the persistent hyperpolarization in L4-SNs is mediated by M_4Rs.

The Persistent Hyperpolarization Is Mediated by Opening of K_{ir} Channels. We next undertook to determine the ion conductance responsible for the M_4R-induced hyperpolarization. Bath applications of ACH invariably elicited an outward current (Fig. 4*A*, *Upper*) correlated with a decrease in input resistance (Fig. 4*A*, *Lower*) in neurons recorded in voltage-clamp (holding potentials −69 to −92 mV; $n = 23$). Moreover, the amplitude of the hyperpolarization was voltage-dependent and reversed at approximately −100 mV ($n = 4$; Fig. 4*B*). We therefore hypothesized that the hyperpolarization is mediated by an increase of a potassium (K^+) conductance. To test this possibility, we used voltage ramps from −44 mV to −134 mV (1 s), before, during and after ACH applications, in the presence of 1 μM TTX. An example of the currents evoked by such voltage ramps is shown in Fig. 4*C*. Subtraction of the current evoked in the presence of ACH from the one evoked in control conditions revealed a current with a strong inward rectification (Fig. 4*C*). Linear fit of this current from −130 to −100 mV gave a reversal potential (−100.7 ± 1.8 mV; $n = 6$) close to the predicted reversal potential for K^+ (−106.3 mV; Nernst equation). The *Inset* in Fig. 4*C* shows the average ACH-induced current of 6 L4-SNs.

These results suggest that the hyperpolarization is mediated by the opening of inwardly rectifying K^+ (K_{ir}) channels (27). Consistently, the hyperpolarization induced by bath and puff applications of 100 μM ACH was blocked by barium (Fig. 4*D*,

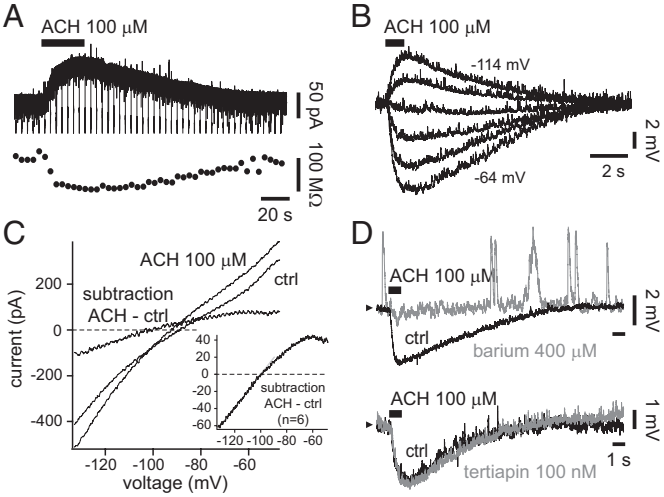

Fig. 4. The persistent hyperpolarization is mediated by the activation of K_{ir} channels. (*A*) Bath application of 100 μM ACH evokes an outward current (*Upper*) correlated with a decrease in input resistance (*Lower*) in a L4-SN recorded in voltage-clamp ($V_{hold} = -92$ mV). (*B*) Voltage-dependence (from −114 to −64 mV by steps of 10 mV) of 100 μM ACH 1-s puffs in a L4-SN recorded in current-clamp. (*C*) Voltage ramps before and after 100 μM ACH evoke different current-voltage relationships (each IV curve is averaged from 3 consecutive ramps) whose subtraction reveals an inwardly rectifying current reversing at ≈−100 mV. *Inset*, average from 6 neurons. (*D*) *Upper*, the hyperpolarization evoked by a 100 μM ACH 1-s puff in control (black trace) is blocked by 400 μM barium (gray trace) in a L4-SN at V_{rest} (arrowhead). *Lower*, 100 nM tertiapin has no effect (gray trace) on the response evoked by a 100 μM ACH 1-s puff in control (black trace) in a L4-SN at V_{rest} (arrowhead). Voltage traces are averages from greater than or equal to 3 trials. In *A–C*, voltages are corrected for the liquid junction potential.

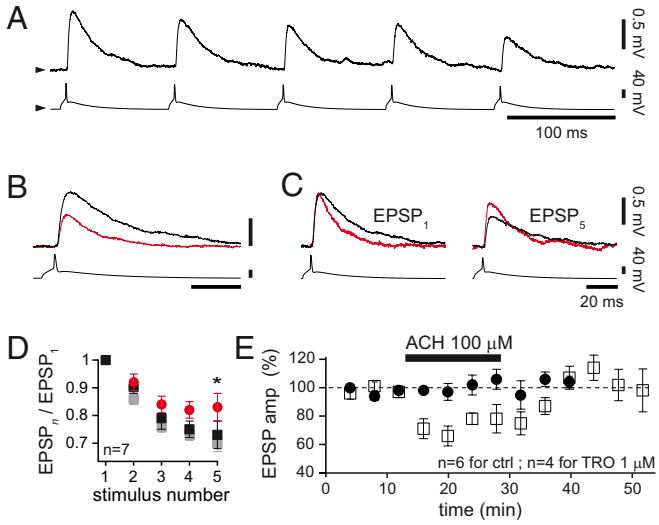

Fig. 5. ACH reduces synaptic efficacy and short-term depression between L4-SNs. (*A*) A train of 5 APs at 10 Hz in a presynaptic L4-SN (*Lower*) evokes EPSPs in a postsynaptic L4-SNs (*Upper*); arrowheads, V_{rest}. (*B*) Bath application of 100 μM ACH (red trace) reduces the amplitude of the evoked EPSPs. (*C*) Scaling the amplitude of the EPSPs obtained in ACH (red) to the first EPSPs amplitude in control (black, $EPSP_1$) reveals a reduction in short-term depression in the fifth EPSP ($EPSP_5$). In *A–C*, same neuron; voltage traces are averages from >35 sweeps and were Y-aligned. (*D*) $EPSP_n/EPSP_1$ ratio (black boxes, control; red circles, 100 μM ACH; gray boxes, wash). (*E*) Time course of the effect of 100 μM ACH on the first EPSP amplitude (white boxes, control; black circles, in the presence of 1 μM TRO).

Upper), a non-specific blocker of K_{ir} channels (barium 200 μM, bath appl., 88.8 ± 6.7% block, $n = 6$; barium 400 μM, puff appl., 91.8 ± 4.6% block, $n = 4$).

To exclude the presence of calcium-activated K^+ channels (10), we tested the effect of ACH on L4-SNs filled with 2 mM BAPTA. These neurons were all hyperpolarized by 100 μM ACH (−3.9 ± 1 mV at V_{rest}, $n = 4$). Finally, since ACH has been shown to activate $K_{ir}3$ channels in the dendrites of hippocampal PCs (28), we tested the effect of tertiapin, a specific blocker of $K_{ir}3$ channels. However, 100 nM tertiapin had no effect on puff applications of 100 μM ACH (mean block −0.1 ± 4.1%, $n = 3$; Fig. 4*D*, *Lower*).

ACH Presynaptically Reduces Synaptic Efficacy in the L4 Recurrent Excitatory Microcircuit. Our results suggest a filtering action of ACH in the L4 recurrent excitatory microcircuit. However, ACH is also known as a powerful modulator of glutamate release in the neocortex. Since the L4-SNs form a recurrent microcircuit with highly reliable connections (21), modulation of synaptic release should have important consequences on their output. Notably, a potentiation of their recurrent synaptic transmission by ACH could counteract the hypothesized filtering action. Therefore, we investigated the effect of ACH on synaptic transmission between pairs of connected L4-SNs at V_{rest}. We used trains of 5 short current stimuli at 10 Hz to evoke APs in the presynaptic neuron (Fig. 5*A*, *Lower*) and their corresponding unitary EPSPs in the postsynaptic neuron (Fig. 5*A*, *Upper*). We found that 100 μM ACH, in addition to its hyperpolarizing effect, significantly and reversibly reduced the amplitude of the first unitary EPSP (−24.3 ± 3.6%, $P < 0.01$, $n = 7$; Fig. 5 *B* and *E*) and significantly and reversibly increased its coefficient of variation (0.28 ± 0.05 in ctrl, vs. 0.37 ± 0.07 in ACH, $P < 0.05$, $n = 7$). ACH also significantly and reversibly reduced short-term synaptic depression (mean $EPSP_5/EPSP_1$ 0.73 ± 0.05 in ctrl, vs. 0.83 ± 0.05 in ACH, $P = 0.02$, $n = 7$; Fig. 5 *C* and *D*). However, there were no significant changes in the EPSP latency and rise time.

To test whether the cholinergic modulation of synaptic transmission is mediated by activation of M_4Rs, we bath-applied 100 μM ACH on neurons preincubated in 1 μM TRO. Under these conditions, ACH had no effect on EPSP amplitude ($P = 0.73$; $n = 4$; Fig. 5*E*) and short-term synaptic depression (for $EPSP_5/EPSP_1$ $P = 0.6$; $n = 4$). These results suggest that ACH reduces release probability in the L4 recurrent excitatory microcircuit through activation of M_4Rs.

Finally, consistent with a filtering action of ACH in the L4 recurrent excitatory microcircuit, we found that 100 μM ACH was also reducing the release probability at the L4-SN to L2/3 PC connection (Fig. S2).

Discussion

This study presents a long-lasting inhibitory effect of ACH, both in response to slow (bath) and fast (puff) changes in the ACH concentration, in a well-defined population of excitatory neurons of the neocortex. We showed that ACH persistently hyperpolarizes L4-SNs in S1 cortex in a dose-dependent manner, through activation of postsynaptic mAChRs, and that this effect is a general feature of sensory cortices. We then demonstrated that the persistent hyperpolarization of neocortical excitatory neurons is specific to L4-SNs and is mediated by M_4R-induced activation of K_{ir} channels. Finally, we demonstrated that ACH presynaptically depresses synaptic transmission in the L4 excitatory microcircuit both at its recurrent synapses (through activation of M_4Rs) and at its output synapses onto L2/3 PCs.

The major finding of this study is that ACH hyperpolarizes the L4-SNs in a persistent manner. This effect is physiologically relevant since the EC_{50} of ACH (6.5 μM), on neurons at membrane potentials (≈ −60 mV) similar to those recorded in awake animals (24), is in the range of the rapid and local changes in neocortical ACH concentrations measured during attentional tasks (29). In previous studies in rodents, a persistent hyperpolarization in response to ACH has only been observed in a few subpopulations of inhibitory neurons of the hippocampus and neocortex (30–32) as well as in extracortical regions of the CNS or in the PNS (33–35). In the neocortex, application of ACH has been reported to invariably induce a persistent depolarization in identified excitatory neurons (9–12).

By directly comparing fast applications of ACH in different layers of S1, we demonstrate that the L4-SNs are always monophasically and persistently hyperpolarized by ACH whereas L2/3 and L5 PCs are always persistently depolarized by ACH. This excludes the possibility that the persistent hyperpolarization is an artifact resulting from our experimental conditions. Moreover, in contrast to earlier studies (10, 12), our results demonstrate that puff applications of ACH induce a monophasic depolarization in the majority of L2/3 and L5 PCs and a biphasic response only in a fraction of these neurons. It is likely that the indirect hyperpolarizing transient due to excitation of GABAergic interneurons in (12) depends on high concentrations of ACH (10 mM), and that the hyperpolarizing transient induced by direct activation of K_{Ca} channels in (10) depends on preceding spiking activity (30). We observed that firing was either required for the transient hyperpolarization or increased its amplitude in both L5 and L2/3 PCs (Fig. S3.). Thus, because i) it is unlikely that volume transmission of ACH reaches concentrations in the millimolar range in vivo, ii) both the spontaneous and sensory-evoked spiking activity of S1 PCs in vivo are low (36–38), iii) only less than half the PCs are transiently hyperpolarized, and iv) the transient hyperpolarization represents only a minor part of the biphasic effect of ACH (≈2.4% of total duration in L5, ≈5.2% in L2/3; ≈21% of peak depolarization in L5, ≈45% in L2/3), we conclude that the effect of ACH is predominantly excitatory in L2/3 and L5 of S1.

The presence of a different mACHR subtype in L4-SNs than in the L2/3 and L5 PCs further supports the idea of a layer-specific effect of ACH. Previous studies showed that both the persistent depolarization and transient hyperpolarization in neocortical PCs were mediated by M_1Rs (10, 12, 39). Our finding of M_4Rs in L4-SNs is consistent with immunohistochemical (40) and in situ hybridization (41) studies showing that M_4Rs are mostly found in L4 while M_1Rs are mostly found in the other layers.

Taken together, our results indicate that ACH has a differential layer-specific effect in S1. It induces a postsynaptic persistent hyperpolarization in the L4-SNs and a postsynaptic persistent depolarization in L2/3 and L5 PCs. It is unlikely that the net effect of ACH release in vivo could excite the L4-SNs through the reduction of an inhibitory tone provided by tonically active GABAergic interneurons. Indeed, most inhibitory inputs received by the L4-SNs originate from GABAergic interneurons that provide a very brief and precisely timed "feed-forward" inhibition (42, 43) and there is no evidence for a tonic inhibition. Furthermore, our results are consistent with in vivo studies (3–5) showing that, while ACH enhances the evoked sensory responses of most neurons located in supra- and infra-granular layers, it inhibits evoked sensory responses of some neurons mainly located at midcortical depths. Notably, one of these studies (3) shows that in S1 the proportion of inhibited neurons is higher in L4 ($\approx$80%) than in the other layers ($\approx$10%).

We conclude that the ACH-induced postsynaptic persistent hyperpolarization of L4-SNs together with the ACH-induced presynaptic depression of their synaptic transmission potently reduce the responsiveness of the L4 recurrent excitatory microcircuit. Such an inhibition challenges the widely accepted concept (15, 16, 44) that ACH enhances sensory processing by an overall excitation of the neocortical excitatory cells. Our results suggest that ACH has a filtering action in the major recipient layer of the neocortex. However, ACH should amplify any input reaching the more integrative layers by increasing the excitability of the PCs. It is tempting to speculate that such a differential layer-specific effect of ACH may contribute to increase the SNR of the cortical responses to sensory inputs. Indeed, in addition to the input-specific effect of ACH that might enhance cortical SNR by favoring thalamocortical inputs over the "intracortical noise" (14), the layer-specific effect demonstrated here might enhance the SNR by filtering out noisy weak thalamocortical inputs in the L4 excitatory microcircuit and by subsequently boosting excitability in L2/3 and L5 excitatory microcircuits. The concept of a cholinergic filtering in the L4-SNs is consistent with the finding that amplification of thalamocortical inputs in the L4 recurrent excitatory microcircuit is not required to drive cortical activity in vivo (45) and supports the hypothesis that the L4 network functions as a damping rather than an amplifying circuit (46).

Finally, our finding that different mACHRs induce inhibition in the L4-SNs and excitation in the L2/3 and L5 PCs might open the door to more specific and/or differential therapeutic strategies to treat cognitive impairments or dysfunctions linked to degeneration of the cholinergic system in pathologies such as Alzheimer's disease and schizophrenia.

Materials and Methods

Acute thalamocortical slices of the barrel cortex (350 μm) were prepared from 18- to 24-day-old Wistar rats as previously reported (21) and immersed under an Olympus or Zeiss microscope equipped for IR-DIC video microscopy. The extracellular solution contained (in mM): 125 NaCl, 2.5 KCl, 25 glucose, 25 $NaHCO_3$, 1.25 NaH_2PO_4, 2 $CaCl_2$, and 1 $MgCl_2$, and was equilibrated with 95% O_2 and 5% CO_2 (pH 7.4; 320 mOsm). Patch pipettes (6–9 MΩ) were filled with a solution containing (in mM): 105 K-gluconate, 30 KCl, and 10 HEPES, 10 phosphocreatine, 4 ATP-Mg, and 0.3 GTP (adjusted to pH 7.3 with KOH; 280 mOsm). Recordings were made at 32–34 °C. Data were acquired at 1–50 kHz after low-pass filtering at 2–5 kHz (Bessel filter) using an EPC10-triple (Heka) or 2 Axopatch 200B amplifiers (Axon). L2/3 and L5 PCs in S1 were chosen into the boundaries of a barrel column and identified by their pyramidal shape and their regular firing pattern. L4-SNs in A1 and V1 were identified by their regular spiking pattern and their localization in the dense granular L4 and/or by the presence of spiny dendrites after Neurolucida reconstruction. Slices containing biocytin-filled (2–3 mg/mL) neurons were processed as previously described (21). For voltage-clamp recordings we used patch pipettes with lower resistance (5–7 MΩ), series resistance compensation (70–80%), and we corrected the voltages for the calculated liquid junction potential (−14 mV).

Pair recordings of connected L4-SNs were obtained and analyzed as described in ref. 21. A baseline was obtained from 30–60 trials in control conditions, then ACH was bath applied for 30–60 trials and was followed by a period of wash of 30–80 trials.

ACH was applied via the bath perfusion system (2.5–4 mL/min) or focally ejected through a patch pipette (tip internal diameter: 1–2 μm) connected to a PDES-02D device (npi). The puff pipette was filled with extracellular solution containing 100 μM ACH, positioned at 10–20 μm from the soma of the recorded cell (always at V_{rest}) and brief (1 s or 10 s) low pressure (0.1–0.5 bar) pulses were applied every 30–60 s. In the absence of pharmacological and electrical manipulations the responses to repeated puffs of ACH did not change during the recording (up to 40 min) and puffs of extracellular solution alone had no effect ($n = 3$). For the experiment with pirenzepine in L5 PCs, a 5-s suprathreshold current pulse, 10–20 s before each puff, was used to increase the transient hyperpolarization.

All data are expressed as mean ± SEM. To assess the differences between control and ACH or ACH and blockers we used the 2-tailed paired Student's *t* test.

ACKNOWLEDGMENTS. We thank M. Mühlethaler, M. Serafin, A. Kerr, S. Williams, and R. Bruno for their comments and W. Hucko for excellent technical assistance. This work was supported by Swiss National Foundation Grant (E.E.), German-Israeli-Foundation Grant I-748–158.1/2002, and the Helmholtz Society.

1. Jones BE (2005) From waking to sleeping: Neuronal and chemical substrates. *Trends Pharmacol Sci* 26:578–586.
2. Himmelheber AM, Sarter M, Bruno JP (2000) Increases in cortical acetylcholine release during sustained attention performance in rats. *Brain Res Cogn Brain Res* 9:313–325.
3. Donoghue JP, Carroll KL (1987) Cholinergic modulation of sensory responses in rat primary somatic sensory cortex. *Brain Res* 408:367–371.
4. Sato H, Hata Y, Masui H, Tsumoto T (1987) A functional role of cholinergic innervation to neurons in the cat visual cortex. *J Neurophysiol* 58:765–780.
5. Sillito AM, Kemp JA (1983) Cholinergic modulation of the functional organization of the cat visual cortex. *Brain Res* 289:143–155.
6. Livingstone MS, Hubel DH (1981) Effects of sleep and arousal on the processing of visual information in the cat. *Nature* 291:554–561.
7. Jacobs SE, Juliano SL (1995) The impact of basal forebrain lesions on the ability of rats to perform a sensory discrimination task involving barrel cortex. *J Neurosci* 15:1099–1109.
8. Prado VF, et al. (2006) Mice deficient for the vesicular acetylcholine transporter are myasthenic and have deficits in object and social recognition. *Neuron* 51:601–612.
9. Desai NS, Walcott EC (2006) Synaptic bombardment modulates muscarinic effects in forelimb motor cortex. *J Neurosci* 26:2215–2226.
10. Gulledge AT, Stuart GJ (2005) Cholinergic inhibition of neocortical pyramidal neurons. *J Neurosci* 25:10308–10320.
11. Kirkwood A, Rozas C, Kirkwood J, Perez F, Bear MF (1999) Modulation of long-term synaptic depression in visual cortex by acetylcholine and norepinephrine. *J Neurosci* 19:1599–1609.
12. McCormick DA, Prince DA (1986) Mechanisms of action of acetylcholine in the guinea-pig cerebral cortex in vitro. *J Physiol* 375:169–194.
13. Dani JA, Bertrand D (2007) Nicotinic acetylcholine receptors and nicotinic cholinergic mechanisms of the central nervous system. *Annu Rev Pharmacol Toxicol* 47:699–729.
14. Hasselmo ME, McGaughy J (2004) High acetylcholine levels set circuit dynamics for attention and encoding and low acetylcholine levels set dynamics for consolidation. *Prog Brain Res* 145:207–231.
15. Krnjevic K (2004) Synaptic mechanisms modulated by acetylcholine in cerebral cortex. *Prog Brain Res* 145:81–93.
16. Rasmusson DD (2000) The role of acetylcholine in cortical synaptic plasticity. *Behav Brain Res* 115:205–218.
17. Gil Z, Connors BW, Amitai Y (1997) Differential regulation of neocortical synapses by neuromodulators and activity. *Neuron* 19:679–686.
18. Hsieh CY, Cruikshank SJ, Metherate R (2000) Differential modulation of auditory thalamocortical and intracortical synaptic transmission by cholinergic agonist. *Brain Res* 880:51–64.
19. Oldford E, Castro-Alamancos MA (2003) Input-specific effects of acetylcholine on sensory and intracortical evoked responses in the "barrel cortex" in vivo. *Neuroscience* 117:769–778.

20. Lübke J, Egger V, Sakmann B, Feldmeyer D (2000) Columnar organization of dendrites and axons of single and synaptically coupled excitatory spiny neurons in layer 4 of the rat barrel cortex. *J Neurosci* 20:5300–5311.
21. Feldmeyer D, Egger V, Lübke J, Sakmann B (1999) Reliable synaptic connections between pairs of excitatory layer 4 neurones within a single 'barrel' of developing rat somatosensory cortex. *J Physiol* 521 Pt 1:169–190.
22. Miller KD, Pinto DJ, Simons DJ (2001) Processing in layer 4 of the neocortical circuit: New insights from visual and somatosensory cortex. *Curr Opin Neurobiol* 11:488–497.
23. Carvell GE, Simons DJ (1990) Biometric analyses of vibrissal tactile discrimination in the rat. *J Neurosci* 10:2638–2648.
24. Crochet S, Petersen CC (2006) Correlating whisker behavior with membrane potential in barrel cortex of awake mice. *Nat Neurosci* 9:608–610.
25. McCormick DA, Prince DA (1985) Two types of muscarinic response to acetylcholine in mammalian cortical neurons. *Proc Natl Acad Sci USA* 82:6344–6348.
26. Caulfield MP, Birdsall NJ (1998) International Union of Pharmacology. XVII. Classification of muscarinic acetylcholine receptors *Pharmacol Rev* 50:279–290.
27. Coetzee WA, et al. (1999) Molecular diversity of K+ channels. *Ann N Y Acad Sci* 868:233–285.
28. Seeger T, Alzheimer C (2001) Muscarinic activation of inwardly rectifying K(+) conductance reduces EPSPs in rat hippocampal CA1 pyramidal cells. *J Physiol* 535:383–396.
29. Parikh V, Kozak R, Martinez V, Sarter M (2007) Prefrontal acetylcholine release controls cue detection on multiple timescales. *Neuron* 56:141–154.
30. Gulledge AT, Park SB, Kawaguchi Y, Stuart GJ (2007) Heterogeneity of phasic cholinergic signaling in neocortical neurons. *J Neurophysiol* 97:2215–2229.
31. McQuiston AR, Madison DV (1999) Muscarinic receptor activity has multiple effects on the resting membrane potentials of CA1 hippocampal interneurons. *J Neurosci* 19:5693–5702.
32. Parra P, Gulyas AI, Miles R (1998) How many subtypes of inhibitory cells in the hippocampus? *Neuron* 20:983–993.
33. Egan TM, North RA (1986) Acetylcholine hyperpolarizes central neurones by acting on an M2 muscarinic receptor. *Nature* 319:405–407.
34. Khateb A, et al. (1997) Modulation of cholinergic nucleus basalis neurons by acetylcholine and N-methyl-D-aspartate. *Neuroscience* 81:47–55.
35. McCormick DA, Prince DA (1986) Acetylcholine induces burst firing in thalamic reticular neurones by activating a potassium conductance. *Nature* 319:402–405.
36. Brecht M, Roth A, Sakmann B (2003) Dynamic receptive fields of reconstructed pyramidal cells in layers 3 and 2 of rat somatosensory barrel cortex. *J Physiol* 553:243–265.
37. de Kock CP, Bruno RM, Spors H, Sakmann B (2007) Layer- and cell-type-specific suprathreshold stimulus representation in rat primary somatosensory cortex. *J Physiol* 581:139–154.
38. Shoham S, O'Connor DH, Segev R (2006) How silent is the brain: Is there a ''dark matter'' problem in neuroscience? *J Comp Physiol A Neuroethol Sens Neural Behav Physiol* 192:777–784.
39. Carr DB, Surmeier DJ (2007) M1 muscarinic receptor modulation of Kir2 channels enhances temporal summation of excitatory synaptic potentials in prefrontal cortex pyramidal neurons. *J Neurophysiol* 97:3432–3438.
40. Levey AI, Kitt CA, Simonds WF, Price DL, Brann MR (1991) Identification and localization of muscarinic acetylcholine receptor proteins in brain with subtype-specific antibodies. *J Neurosci* 11:3218–3226.
41. Buckley NJ, Bonner TI, Brann MR (1988) Localization of a family of muscarinic receptor mRNAs in rat brain. *J Neurosci* 8:4646–4652.
42. Porter JT, Johnson CK, Agmon A (2001) Diverse types of interneurons generate thalamus-evoked feedforward inhibition in the mouse barrel cortex. *J Neurosci* 21:2699–2710.
43. Gabernet L, Jadhav SP, Feldman DE, Carandini M, Scanziani M (2005) Somatosensory integration controlled by dynamic thalamocortical feed-forward inhibition. *Neuron* 48:315–327.
44. Detari L, Rasmusson DD, Semba K (1999) The role of basal forebrain neurons in tonic and phasic activation of the cerebral cortex. *Prog Neurobiol* 58:249–277.
45. Bruno RM, Sakmann B (2006) Cortex is driven by weak but synchronously active thalamocortical synapses. *Science* 312:1622–1627.
46. Pinto DJ, Hartings JA, Brumberg JC, Simons DJ (2003) Cortical damping: Analysis of thalamocortical response transformations in rodent barrel cortex. *Cereb Cortex* 13:33–44.